Available online at www.sciencedirect.com

ScienceDirect

Procedia Engineering 64 (2013) 497 – 506

Procedia Engineering

www.elsevier.com/locate/procedia

International Conference On DESIGN AND MANUFACTURING, IConDM 2013

CFD Analysis of Combustion and Pollutant Formation Phenomena in a Direct Injection Diesel Engine at Different EGR Conditions

R. Manimaran[a], R. Thundil Karuppa Raj[b]*

[a]*Thermal & Automotive Division, School of Mechanical & Building Sciences, VIT University, Vellore-632014, Tamil Nadu, India*
[b]*Energy Division, School of Mechanical & Building Sciences, VIT University, Vellore-632014, Tamil Nadu, India*

Abstract

In this work, exhaust gas recirculation (EGR) is varied in a direct injection constant speed diesel engine using extended coherent flame model for 3-zones by CFD. The three zones are unmixed fuel zone, mixed gases zone, unmixed air plus EGR zone. The three zones are too small to be resolved by the mesh and are therefore modeled as sub-grid quantities. The mixed zone is the result of turbulent and molecular mixing between gases in the other two zones, where combustion takes place. Grid and time independent tests are carried out further to find the appropriate space and time steps respectively. The preliminary studies are carried out to validate the model with the experiments. The present study is conducted towards varying the EGR in the cylinder. CFD results indicate that as EGR increases, nitrogen oxides decreases in a general trend observed in diesel engines. The predicted model shows that flame temperature is lowered in the combustion chamber with the increase in EGR. However, as oxides of nitrogen decreases, soot increases due to lowered oxygen concentration. Reaction variable and temperature contours in the cylinder reveal that combustion regresses as EGR is increased.

Selection and peer-review under responsibility of the organizing and review committee of IConDM 2013

Keywords: Direct injection diesel engine; Exhaust Gas Recirculation (EGR); Computational Fluid Dynamics (CFD); Extended Coherent Flame Model; Combustion; Emissions

Nomenclature

3Z	3 Zones
k	Turbulence kinetic energy (m^2/s)
BDC	Bottom Dead Centre
CA	Crank Angle (^{o} or deg)
CD	Computational Dynamics
CFD	Computational Fluid Dynamics
CO	Carbon mono oxide
C_p	Specific heat at constant pressure
C_v	Specific heat at constant volume
ECFM	Extended Coherent Flame Model
EGR	Exhaust Gas Recirculation
HC	Hydrocarbons
N	Engine speed (RPM)
NO_x	Oxides of nitrogen (g/kg of fuel)
P	Cylinder Pressure (bar)

* Corresponding author. Tel.: +91-9444142658;
E-mail address: thundilr@gmail.com

Selection and peer-review under responsibility of the organizing and review committee of IConDM 2013
doi:10.1016/j.proeng.2013.09.124

PISO	Pressure Implicit by Splitting of operators
Q	Heat release rate (J/deg)
RNG	Re-Normalization Group
SMD	Sauter Mean Diameter (m)
STAR	Simulation of Turbulence in Arbitrary Regions
T	Temperature (K)
TDC	Top Dead Centre
V	Cylinder volume
Greek symbols	
ε	Turbulence dissipation rate (m^2/s^3)
γ	Ratio of specific heats (C_p/C_v)
θ	Crank angle (deg)

1. Introduction

Lean fuel operation and high compression ratio favor diesel engines to result in high thermal efficiencies. The high compression ratio produces the high temperatures required to achieve auto-ignition, and the resulting high expansion ratio makes the engine discharge less thermal energy in the exhaust. The extra oxygen in the cylinders is necessary to facilitate complete combustion and to compensate for non-homogeneity in the fuel distribution. Although simultaneous advantage between power and emission cannot be obtained, trade-off between the power output and the NO_x emissions is better achieved using controlled feedback injection timing [1] mainly in compression ignition engines. The time period between the spray of diesel fuel and actual start of combustion is generally referred as ignition delay period. This ignition delay period is a crucial task during experimental investigation of diesel engines. The study of these processes by experimental approach involves expensive instruments with high level of skill and moreover, consumes a lot of time. Nowadays computational techniques evolved such that modeling these processes can contribute to better understanding of spray penetration, combustion and pollutant formation.

An eulerian-lagrangian spray and atomization model for diesel sprays was proposed successfully by Reitz & Diwakar [2]. Their numerical study on internal flow characteristics for a multi-hole fuel injector gives better agreement with the available experimental data. This indicates the capability of numerical model for studying diesel spray characteristics. Magnussen et al. [3] developed a model based on the eddy break-up concept. This model relates the combustion rate to the eddy dissipation rate. This model expresses the rate of reaction by the mean mass fraction of the reacting species, the turbulence kinetic energy and the rate of dissipation.

The spray penetration in the combustion chamber by accompanying different spray droplet break up due to instability was performed by Hossainpour and Binesh [4]. The spray calculations are based on statistical method referred as discrete droplet method. The results are validated with the experimental data. They reported that spray penetration which plays a dominant role in combustion and emission characteristics are predicted better with modeling methodologies. Prasad et al. [5] carried out simulation on different bowl configuration to analyze the effect of swirl on combustion. They found that re-entrant piston bowl could create highest turbulent kinetic energy and swirl in the cylinder. They also studied the effects of injector sac volume on the combustion and emission. The studies indicate that sac-less injector could result in lower emissions. Many literature [6-10] insist that spray dynamics plays a strong role on evaporation rate, flow field, combustion, thermodynamics, heat transfer processes and pollutant formation. As a result, the atomization of fuel affects the combustion efficiency and pollutant formation. Modeling the atomization process during diesel combustion requires careful validation with the experimental results.

Various models are studied [11-14] for optimizing the combustion processes by stochastic procedures. Swirl is varied by designing the intake port and shaping the piston bowl for re-entrant combustion. For combustion chamber of re-entrant effects, the turbulent kinetic energy is intensified at TDC of compression stroke due to the conservation of angular momentum. Combustion is efficient and leads to low soot and high NO_x emissions. The effect of variation of injection timing in diesel engine was studied by Sayin & Canakci [15]. They found that NO_x and carbondioxide emissions increased while the unburned HC & CO emissions decreased when injection timing is advanced. Han et al. [16] investigated numerically the multiple injections and split injection cases. They found that split injection reduces the soot significantly without the change in NO_x emissions whereas multiple injections reduce NO_x significantly. The numerical study on diesel engine simulation with respect to injection timing and the air boost pressure was carried out by Jayashankara et al. [17]

using commercial CFD code. They validated the results of flow-field from CFD simulation with the experimental work of Payri et al [18]. From the CFD simulation, they observed that increase in cylinder pressure, cylinder temperature and NO_x emissions results from advancing the injection timing. They also found from simulation that the supercharged and inter-cooled engine results in higher NO_x emissions as compared to naturally aspirated engines.

An advanced version of combustion model, named as ECFM-3Z model is accompanied in this present work to predict the parameters of flow field and combustion and regarding the pollutant formation processes. This model includes 3-zone modeling with the inclusion of EGR. The code used involves the study of droplet parameters towards combustion and emissions that are rarely reported in literature due to the difficulty in experimental measurements. This gives us the opportunity and motivation to study the droplet variables, combustion and emission characteristics by varying the EGR quantity. It is found that CFD modeling gives better understanding on the processes to study the droplet variables on the variation of EGR.

2. CFD Models

The modeling of flow field of continuous and dispersed phases, combustion and pollutant formation are carried out in detail using a commercial CFD package, STAR-CD. The three dimensional in-cylinder, transient and reacting flow system in a direct injection Diesel engine is modelled by solving a set of governing equations from the law of conservation of mass, momentum, energy and species.

2.1 Turbulence Modeling

The in-cylinder flow is turbulent in nature at all speeds and dimensions of the engine. It is necessary to model the turbulence to capture the properties of in-cylinder fluid dynamics. The RNG k-ε model [21] is which the turbulent Reynolds number forms of the k and ε equations are used in conjunction with the algebraic 'law of the wall' representation of flow, heat and mass transfer for the near wall region.

2.2 Combustion & Ignition Models

The ECFM-3Z model [22] is a general purpose combustion model capable of simulating the complex mechanisms of turbulent mixing, flame propagation, diffusion combustion and pollutant emission that characterize modern internal combustion engines. It can also be used for in-cylinder analysis in a multi-injection environment and for multi-cycle simulations. '3Z' stands for three zones of mixing, namely the unmixed fuel zone, the mixed gases zone, and unmixed air plus EGR zone. The three zones are too small to be resolved by the mesh and are therefore modeled as sub-grid quantities. The mixed zone is the result of turbulent and molecular mixing between gases in the other two zones and is where combustion takes place.

2.3 Droplet Models

Droplets from the nozzle enters the combustion chamber at high velocity and gets sheared at the outer periphery. Hence a model to disintegrate the droplets is given by Reitz and Diwakar model [2]. Huh's model [25] is based on the gas inertia and the internal turbulence stresses generated in the nozzle. The Bai [24] spray impingement model is formulated within the framework of the lagrangian approach in order to reflect the stochastic nature of the impingement process, a random procedure is adopted to determine some of the droplet post-impingement quantities. This allows secondary droplets resulting from a primary droplet splash to have a distribution of sizes and velocities.

2.4 Pollutant Formation Models

Nitrogen oxides (NO_x) are important air pollutants, mainly produced by combustion devices. The NO_x concentration is low in most of these devices; therefore, it has little influence on the flow field. Also, the time scale for NO_x reactions [29] is larger than the time scales for the turbulent mixing process and the combustion of hydrocarbons that control the heat-releasing reactions. Hence, computations of NO_x can be decoupled from the main reacting flow field predictions by identifying three different mechanisms for the formation of nitric oxide during the combustion of hydrocarbons. The formation and emission of carbonaceous particles is a process that is often observed during the combustion of hydrocarbons. These particulates, called soot, are identified in flames and fires as yellow luminescence. One class of modeling soot formation is based on specifying detailed reaction mechanisms for the gas phase chemistry and the formation, growth and oxidation of soot particles. The first approach, due to Mauss [30] and his colleagues, is based on the laminar flamelet

concept in which all scalar quantities are related to the mixture fraction and scalar dissipation rate. Whereas the species mass fractions are unique functions in the mixture fraction-scalar dissipation space, the soot mass fractions are not. The rates of soot formation can, however, be correlated with local conditions in diffusion flames or in partially premixed counter-flow twin flames.

3. Computational Procedure

3.1 Mesh Generation

CFD simulation starts with the geometry of the piston bowl, referred from Colin et al [22]. The piston bowl shape is prepared from a standard computer-aided-design package. After the piston bowl is generated [19], a spline is created from the bowl profile and used for the creation of in-cylinder mesh. The meshing of the in-cylinder fluid domain is performed using *es-ICE* (*Expert System – Internal Combustion Engine* [27]) grid generation tool. In this study, a 45^{o} sector mesh is considered due to symmetry nature of the in-cylinder domain and thereby the computational time can be reduced considerably. The in-cylinder grid thus obtained is checked for negative volumes at all locations between BDC and TDC. The meshed geometry of the moving fluid domain at TDC i.e. 720 deg CA is shown in Fig 1 and contains almost hexahedral and tetrahedral cells near cylinder axis.

Fig. 1. Computational grid with boundary surfaces at 720 ^{o}CA (TDC)

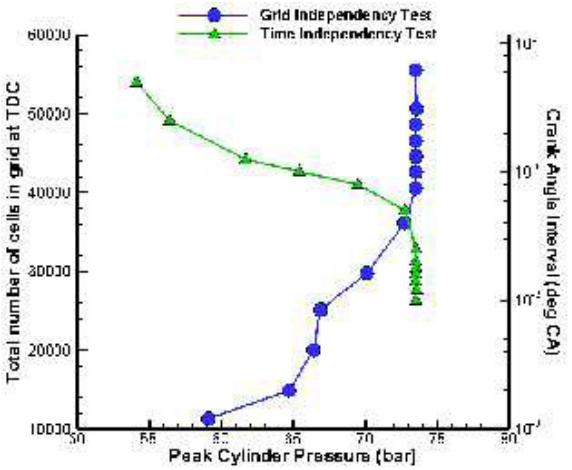

Fig. 2. Variation of peak pressure with grid density & crank angle interval

3.2 Boundary Conditions

The boundary conditions involved in the in-cylinder fluid domain have to be supplied to facilitate the solution of energy and momentum conservation equations. The boundary of the domain consists of moving wall at the bottom, periodic zones at the sides, cylinder liner wall, cylinder head wall at the top, axis and the injector. Piston top wall is applied with the moving wall boundary condition. The velocity of piston wall is calculated using the engine speed, crank angle, connecting rod and stroke length details. The other surfaces of the geometry are simply stationary walls i.e. no slip condition. The different temperatures obtained from experiments at various surfaces are listed in Table 1.

3.3 Convergence Criteria

The continuity, momentum, energy and species equations are solved for every time step with convergence requirement of 1E-05. In this numerical study, the transient simulation starts at 680^{o}CA and ends at 800^{o}CA. This is the crucial period of investigation towards combustion and pollutant formation. For every time step, convergence conditions have to be met for all the equations.

3.4 Grid and Time Independency Tests

The grid and time independent tests are carried out as shown in Fig. 2. It can be observed from Fig. 2 that increasing the cells beyond 45000 cells does not alter the in-cylinder peak pressure and other process variables. Thus the grids that are solved by finite volume method are independent beyond 45000 cells at TDC location. It can be observed that in-cylinder

averaged peak pressure does not get varied even the crank angle step interval is reduced below 0.025 deg. Hence the optimum crank angle step interval is maintained at 0.025 deg for all simulations in this study.

3.5 Solver Details

Lagrangian multiphase treatment is activated in the simulation of droplet break-up and spray penetration phenomena. The turbulent dispersion model is included for the droplet to experience randomly varying velocity field in the cylinder. Collision model [20] is also considered to detect the collision of parcels for every time step. Gravitational force is also accounted on the droplet parcels. The number of droplet parcels considered in this work is exceeded beyond 50 million in numbers that enables to study the trajectory, spray penetration and collision physics. RNG k-ε turbulence model [21] is used for modeling the turbulent eulerian flow-field in the cylinder. The flame surface density equation is solved by adopting extended coherent flame model for 3 zones namely, the unmixed fuel zone, the mixed gases zone and the unmixed zone of air together with EGR [22].

The ECFM-3Z combustion model [22] is chosen for the simulation of complex mechanisms like turbulent mixing, flame propagation, diffusion combustion and pollutant formations. A small amount of exhaust gas is mixed with fresh air and then introduced into the combustion chamber. This modifies the fuel/air ratio and EGR, which lowers the peak temperature so that the chemical reaction rate between nitrogen and any unused oxygen is strongly reduced. Species concentrations involved in combustion reactions can be written as a function of mixture fraction within the presumed probability density function model of combustion. Table 2. lists the models accompanied in the code for simulation. The liquid film model [23] accounts for convective transport of conserved quantities within the film and from/to the gas phase. Spray impingement model [24] is formulated within the framework of the Lagrangian approach to reflect the stochastic nature of the impingement process. A random procedure is adopted to determine the droplet post-impingement quantities. This allows secondary droplets resulting from a primary droplet splash to have a droplet size and droplet velocity distributions. The standard pool boiling [26] is used to model liquid film boiling, when the wall temperature exceeds the saturation temperature of the liquid as the film starts to boil when the heat flux passes from the wall to the film. The injections of fuel start at 714° which is equal to 6° before TDC. The injection of droplets at three crank angles viz. 718° CA to 720° CA are as shown in Fig. 3 (a), (b) and (c) respectively. The breakup of spray as observed in Fig. 3 is common in diesel engines due to surface tension and aerodynamic shear between the fuel and surrounding air in turbulent motion inside the cylinder at high pressures.

Table 1. Boundary Conditions

Boundary	Momentum boundary condition	Thermal boundary Condition [22]
Cylinder head	Wall	450 K
Cylinder wall	Wall	400 K
Piston bowl	Moving wall	450 K
Cylinder side face	Periodic	450 K

Table 2. Models accompanied in STAR-CD code

Phenomena	Model
Droplet breakup	Reitz-Diwakar [2]
Turbulence	RNG k-ε model [21]
Combustion	ECFM-3Z compression [22]
Liquid Film	Angelberger [23]
Droplet wall interaction	Bai [24]
Atomization	Huh [25]
Boiling	White [26]
NO_x mechanism	Hand [28], De Soete [29]
Soot	Mauss [30]

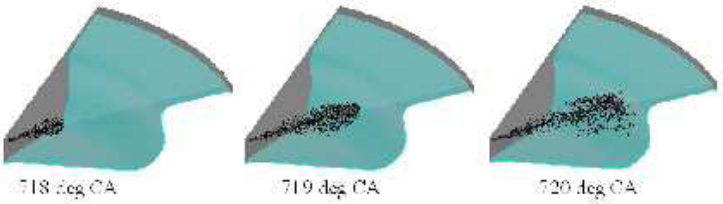

(a) (b) (c)

Fig. 3. Spray Evolution : (a) 2°CA before TDC, (b) 1°CA before TDC and (c) at TDC (720 °CA)

Solver parameters considered in this work are *cylinder pressure, cylinder temperature, heat release rate, reaction variable, droplet diameter (SMD), NO_x, soot* and *CO*. The STAR-CD [27] code computes by discretizing the fluid domain using finite

volume approach under implicit formulation mode. The PISO algorithm is used to provide pressure velocity coupling to compute the flow-field and other transport equations (species and flame surface density). Second order upwind scheme is employed to discretize the conservation equations of mass, momentum and energy. Lagrangian equations, when integrated over the control volume, yield the changes in the momentum, mass and energy of each discrete element between its entry and exit. The sum of these changes for all elements crossing the volume provides the net momentum, mass and energy exchanged with the carrier fluid.

3.6 Post-Processing

Time step computations are carried out till the residual values of the conservation equations of continuity, momentum and energy fall below 10^{-5}. Auxiliary equations involving the turbulence, spray models and models for combustion and soot emissions are also computed at every time step. Once a time step is completed, the code outputs the in-cylinder averaged data such as pressure, temperature, heat release rate, NO_x and soot emissions to an ASCII file output for further analysis. The contours of the same quantities are also obtained by storing the information at preset crank-angles.

4. Validation

To verify the results from the simulation, the pressure data computed is compared against experimental pressure data from literature [22]. Table 3. shows the specification of engine dimensions, injection timing and combustion parameters. The 45° sector CFD model of Colin et al. [22] experimental engine cylinder is modeled and a series of grid and time independency tests are carried out as shown in Fig. 2. Crank angle step interval of 0.025° CA (i.e. 4.167 x 10^{-6} seconds) and mesh with 45000 cells (at TDC) are obtained as key information for further simulation from these tests. Validation of the current simulation work is carried out with the experimental pressure data of Colin et al. [22] from the literature. Fig. 4 shows the comparison of the simulation results with the experimental in-cylinder pressure under firing conditions. The computed in-cylinder pressure data from numerical simulation are in good agreement with the experimental data. The in-cylinder averaged pressure during the non-firing mode of simulation is also shown in Fig. 4. The numerically simulated pressure values are in close agreement with the experimental data and the maximum deviation in peak pressure is less than 0.2%.

Table 3. Engine specifications

Bore	0.085 m
Stroke	0.088 m
Compression ratio	18
Connecting Rod Length	0.145 m
Valves/Cylinder	4
Engine Speed (N)	1640 RPM
Fuel	n-Dodecane
Start of injection	6.0 °CA bTDC
Injection duration	8.03 °CA
Injected mass	0.0144 g
Fuel-air equivalence ratio	0.67
EGR rate (%)	31
Swirl ratio	2.8
Injector hole diameter	148 x 10^{-6} m
Spray angle	152 deg
Intake valve opening (lift at 0.5 mm)	360 deg (TDC)
Intake valve closing (lift at 0.5 mm)	574 deg
Exhaust valve opening (lift at 0.5 mm)	860 deg

5. Results and Discussion

In-cylinder parameters such as pressure, temperature, heat release rate, NO_x and soot emissions are predicted numerically for the same geometry of Colin et al. [22]. EGR is varied from 0 % to 30 %. This is normally achieved in a heavy duty direct injection Diesel engine. The in-cylinder pressure increases till 736 deg CA in Fig. 5 due to diffusion combustion and thereafter decreases as expected. It is found that the peak pressure during the simulation reaches nearly 84 bar at nearly 740° CA for 0 % EGR. At 30 % EGR, the incylinder pressure drops to 75 bar. The presence of EGR in the cylinder (i.e given as initial condition in this simulation) decreases the reaction in the cylinder as shown in the Fig. 6. As EGR increases, the

reaction variable is reduced considerably at certain locations in the combustion chamber as shown in Fig. 6 when the piston is at TDC. The contours are obtained at 1 mm below the cylinder head.

$$\frac{dQ}{d\theta} = \frac{1}{\gamma - 1} V \frac{dp}{d\theta} + \frac{\gamma}{\gamma - 1} P \frac{dV}{d\theta} \qquad (1)$$

Heat release in the cylinder is due to increase in pressure and temperature as given by first law of thermodynamics in Eq. (1). The in-cylinder heat release rate curve rises after 716 deg CA steeply due to the rapid rise in pressure. During this period, the mixture may be homogeneous such that premixed combustion can happen. Due to the sudden rise in pressure, the firing inside the cylinder leads to uncontrolled combustion. After the peak heat release, the combustion is controlled due to diffusion between air and fuel particles. Fig. 5 also shows the heat release rate for different EGR conditions. Since the peak pressure is reduced at higher EGR level, the heat release rate is significantly reduced from 41 J/deg CA to 32 J/deg CA with a reduction of 28 % heat release in J/deg CA. The reaction variable contours (Fig. 6) give clear understanding of burnt and unburnt locations. All the contours are shown at TDC, sliced at 1 mm below the cylinder head. Reaction variable of 0 denotes the fuel is unburnt completely i.e. near cylinder wall whereas reaction variable with a value of 1 denotes the fuel is burnt completely near the injector and above the bowl edge. The bowl presents a tumble motion that enables the acceleration of mixing between fuel and air near this place and further auto-ignition. Table 4. lists the ignition delay for various EGR conditions. Since the combustion is regressive at higher EGR levels, the ignition delay is increased from 3.07 deg CA to 4.35 deg CA.

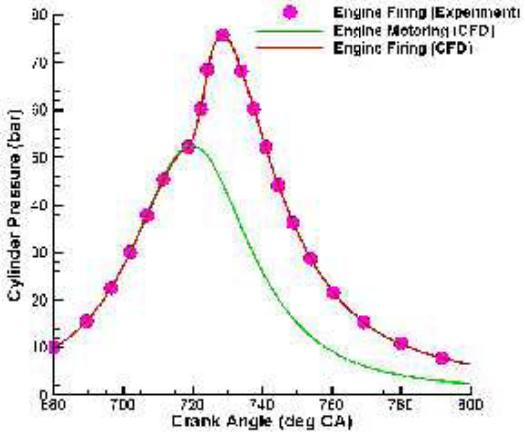

Fig. 4. Comparison of computed and experimental Pressure data with crank angle

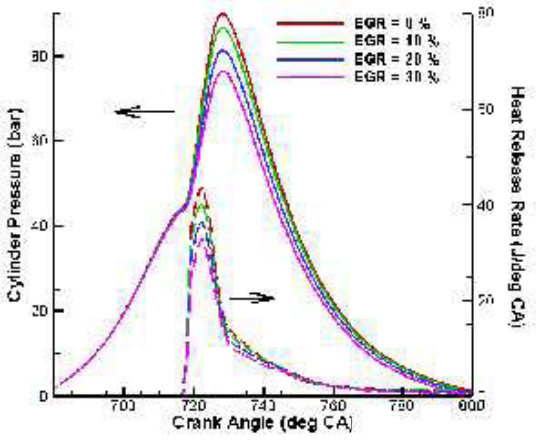

Fig. 5. Variation of pressure & heat release rate with crank angle at different EGR

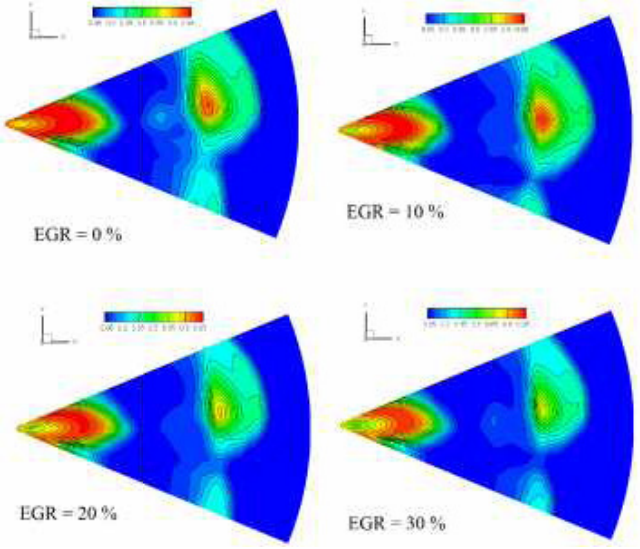

Fig. 6. Contours of reaction variable at 720 ^{o}CA

The in-cylinder temperature is plotted for different EGR levels in Fig. 7. It can be observed that peak cylinder temperature drops from 1750 K to 1500 K as EGR is increased from 0 % to 30 %. The temperature contours are also shown in Fig. 8. It can be observed that the cylinder temperature is lowered as EGR is increased. NO_x plots in the Fig. 7 indicate the reduction of nitrogen oxide levels from 12 g/kg of fuel to 3 g/kg of fuel. NO_x increases as the peak temperature rises due to the thermal NO_x formation.

Table 4. Ignition delay for various EGR

EGR (%)	Ignition Delay (^{o} CA)
30	4.35
20	3.97
10	3.55
0	3.07

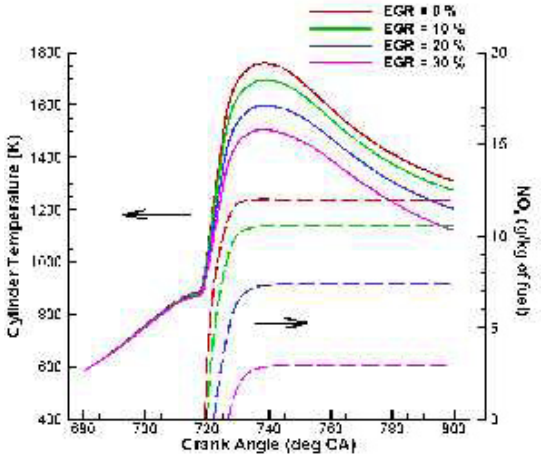

Fig. 7. Variation of Cylinder temperature, NO_x for different EGR

Fig. 9 shows the soot and droplet SMD variations for a part of the expansion or power stroke. The soot levels rise from 0.17 g/kg of fuel to 0.25 g/kg of fuel. This is due to improper combustion as the reaction is regressed when EGR is increased. The droplet diameter typically Sauter Mean Diameter increases from 240 microns to 260 microns due to coalescence in the Fig. 9 as EGR is increased. The soot level rises up earlier than 720^o CA while NO_x emissions rise little later than 720^o CA. Soot is formed from unburned fuel that nucleates from the vapor phase to a solid phase in fuel-rich regions at elevated temperatures. Hydrocarbons or other available molecules may condense on, or be absorbed by soot depending on the surrounding conditions. The fuel droplet traces a nearly linear path from the time of formation, often breaking and coalescing with other drops in the neighbourhood. The coalescence is however not applicable to the drops on the outer envelope of spray because the droplets are formed first and hence do not interact with other droplets on the outside. The trajectory and breakup of droplet depends on ambient pressure, neighbourhood velocity too. Break-up of these drops is negligible if the drops are small as in high-pressure sprays. Thus, the droplets on the spray surface can be said to reduce in

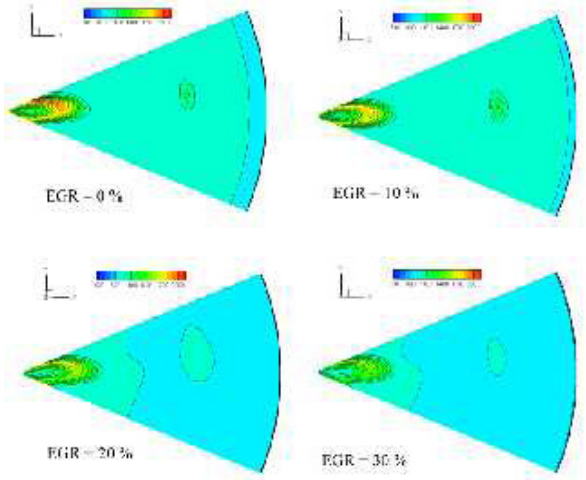

Fig. 8. Contours of temperature (K) at 720 ^{o}CA

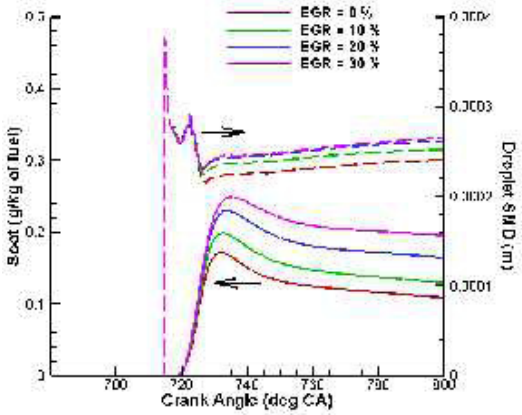

Fig. 9. Variation of droplet SMD & soot for different EGR

size only by vaporisation. Evaporation of fuel depends on the temperature and relative velocity between droplet and continuous phase medium. The CO contours are shown in Fig. 10 that exhibit a increasing trend with EGR. CO results from incomplete combustion in the cylinder and it increases as EGR is increased.

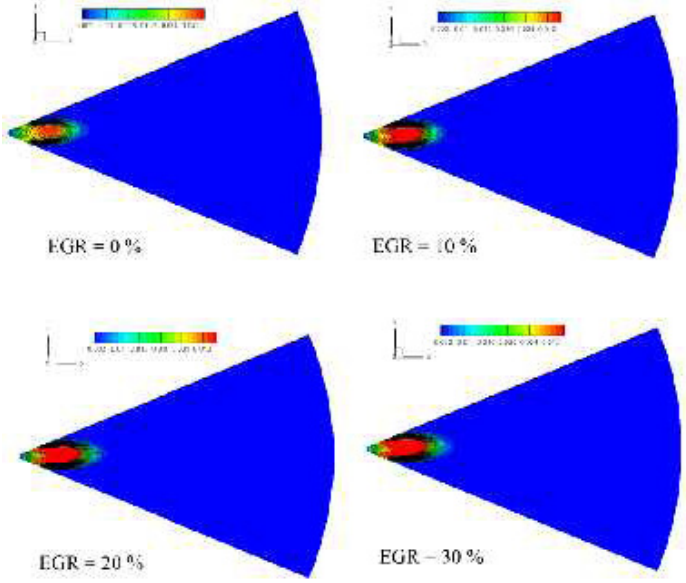

Fig. 10. Contours of CO (mass fraction) for different EGR at 720 ^{o}CA

6. Conclusion

In the present work, several models governing the direct injection diesel engine combustion and pollutant formation are presented and studied. The results from the simulation are validated after the grid and time independency tests are performed. From the variation of EGR in the simulation, the following conclusions are obtained.

1. When the EGR is increased from 0 % to 30 %, the peak in-cylinder pressure decreases by 9 bar thereby resulting in regressive combustion.
2. Heat release occurs nearly at 722 deg CA and increases by 28 % when EGR is decreased from 30 % to 0 %.
3. There is 14.3 % reduction in peak cylinder temperature as EGR is lowered from 30 % to 0 %. The decrease in cylinder temperature brings down the NO_x emissions by 75 %.
4. Droplet SMD is increased by 9.2 % and soot level increases by 41.2 % as EGR is increased from 0 % to 30 %.

References

[1] Heywood, J. B., 1988. International combustion engine fundamentals, McGraw-Hill, Newyork, p. 491-566.
[2] Reitz, R.D., Diwakar, R., 1986. Effect of drop breakup on fuel sprays, SAE Technical Paper Series, 860469.
[3] Magnussen, B.F., Hjertager, B.H., 1976. On mathematical modeling of turbulent combustion with special emphasis on soot formation and combustion, 16th Symp. on Combustion, The Combustion Institute, p. 719-729.
[4] Hossainpour, S., Binesh, A.R., 2009. Investigation of fuel spray atomization in a DI heavy-duty diesel engine and comparison of various spray breakup models, Fuel 88, p. 799-805.
[5] Prasad, B.V.V.S.U., Sharma, C.S., Anand, T.N.C., Ravikrishna. R.V., 2011. High swirl-inducing piston bowls in small diesel engines for emission reduction, Applied Energy 88, p. 2355-2367.
[6] Baker, D.M., Assanis D.N., 1994, A methodology for coupled thermodynamic and heat transfer analysis of a diesel engine, Applied Mathematical Modelling, 18(11), p. 590-601.
[7] Qi, K., Feng, L., Leng, X., Du, B., Long, W., 2011. Simulation of quasi-dimensional combustion model for predicting diesel engine performance, Applied Mathematical Modelling, 35(2), p. 930-940.
[8] Park, K., Wang, D.M., Watkins, A.P., 1993. A contribution to the design of a novel direct- injection diesel engine combustion system— analysis of pip size, Applied Mathematical Modelling, 17(3), p. 114-124.
[9] Tanner, F.X., Srinivasan, S., 2009. CFD-based optimization of fuel injection strategies in a diesel engine using an adaptive gradient method, Applied Mathematical Modelling, 33(3), p. 1366-1385.
[10] Watkins, A.P., Khaleghi, H., 1990. Modelling diesel spray evaporation using a noniterative implicit solution scheme, Applied Mathematical Modelling, 14(9), p. 468-474.
[11] Lino, P., Maione, B., Rizzo, A., 2007. Nonlinear modelling and control of a common rail injection system for diesel engines, Applied Mathematical Modelling, 31(9), p. 1770-1784.
[12] Payri, F., Benajes, J., Tinaut, F.V., 1988. A phenomenological combustion model for direct-injection, compression-ignition engines, Applied Mathematical Modelling, 12(3), p. 293-304.
[13] Dhuchakallaya, I., Watkins, A.P., 2010. Auto-ignition of diesel spray using the PDF-Eddy Break-Up model, Applied Mathematical Modelling, 34(7), p. 1732-1745.
[14] Kondoh, T., Fukumoto, A., Ohsawa, K., Ohkubo, Y., 1985. An assessment of a multidimensional numerical method to predict the flow in internal combustion engines, SAE Paper 850500.
[15] Cenk Sayin, Mustafa Canakci, 2009. Effects of injection timing on the engine performance and exhaust emissions of a dual- fuel diesel engine, Energy Conversion & Management, 50,p. 203–213.
[16] Han Z., Uludogan, A., Hampson, G.J., Reitz, R.D., 1996. Mechanism of soot and NO_x emission reduction using multiple-injection in a diesel engine, SAE paper 960633.
[17] Jayashankara, B., Ganesan, V., 2010. Effect of fuel injection timing and intake pressure on the performance of a DI diesel engine – A parametric study using CFD, Energy Conversion and Management, 51, p. 1835–1848.
[18] Payri, F., Benajes, J., Margot, X., Gil, A., 2004. CFD modeling of the in-cylinder flow in direct-injection diesel engines, Computers & Fluids, 33, p. 995–1021.
[19] Béard, P., Colin, O., Miche, M., 2003. Improved modeling of DI Diesel engines using sub-grid descriptions of spray and combustion, SAE Paper 2003-01-0008..
[20] O'Rourke, P.J., 1981. Collective Drop Effects on vaporising Liquid Sprays, PhD Thesis, University of Princeton.
[21] El Tahry, S.H.,1983. k-ε equation for compressible reciprocating engine flows, AIAA, J. Energy 7, p. 345–353.
[22] Colin, O., Benkenida, A., 2004. The 3-Zone Extended Coherent Flame Model (ECFM3Z) for computing premixed/diffusion combustion, Oil & Gas Science and Technology – Rev. IFP, 59, p. 593-609.
[23] Angelberger, C., Poinsot, T., Delhay, B., 1997. Improving near-wall combustion and wall heat transfer modeling in SI Engine Computations, SAE Technical Paper Series 972881, p. 113-130.
[24] Bai, C., Gosman, A.D., 1996. Mathematical modeling of wall films formed by impinging sprays, SAE Technical Paper Series 960626.
[25] Huh, K.Y., Gosman, A.D., 1991. A phenomenological model of Diesel spray atomisation', Proc. Int. Conf. on Multiphase Flows (ICMF '91), Tsukuba,
[26] Rohsenow, W.M., 1952, A method of correlating heat transfer data for surface boiling liquids, Transactions of the ASME, 74, p. 969.
[27] CD-Adapco version 4.16, 2010. STAR methodology for internal combustion engine applications.
[28] Hand, G., Missaghi, M., Pourkashanian, M., Williams, A., 1989. Experimental studies and computer modelling of nitrogen oxides in a cylindrical natural gas fired furnace, 9th Members Conf., International Flame Research Foundation, Noordwijkerhout, The Netherlands.
[29] De Soete, G.G., 1975. Overall reaction rates of NO and N_2 formation from fuel nitrogen, 15th Symp. (Int.) on Combustion, The Combustion Institute, p. 1093-1102.
[30] Mauss, F., Netzell, K., Lehtiniemi, H., 2006. Aspects of modeling soot formation in turbulent diffusion flames, Combust. Sci. and Tech., 178, p. 1871.